

# Fatigue Analysis of Spot-Welded Automobile Components Considering Fatigue Damage-Induced Stiffness Degradation in Time and Frequency Domains

Jae-Hoon Kim<sup>1</sup>, Dong-Chul Lee<sup>2</sup>, Jang-Ho Lee<sup>3</sup>, Young-Sam Ham<sup>1</sup>, and Ki-Weon Kang<sup>3#</sup>

<sup>1</sup> High Speed System Research Center, Korea Railroad Research Institute, 176, Cheoldobangmulgwan-ro, Uiwang-si, Gyeonggi-do, 16105, South Korea

<sup>2</sup> Kunsan Automobile Technology Innovation Center, Kunsan National University, 558, Daehak-ro, Gunsan-si, Jeollabuk-do, 54150, South Korea

<sup>3</sup> School of Mechanical Engineering, Kunsan National University, 558, Daehak-ro, Gunsan-si, Jeollabuk-do, 54150, South Korea

# Corresponding Author / E-mail: kwkang68@kunsan.ac.kr; TEL: +82-63-469-4872, FAX: +82-63-469-4727

KEYWORDS: Fatigue damage-induced stiffness degradation, Multi-point spot-welded structure, Quasi-static fatigue analysis, Vibration fatigue analysis

*In this study, fatigue analysis was performed on a multi-point spot-welded outrigger structure utilized in an automobile engine room, where stiffness degradation from accumulated fatigue damage were considered. The S-N curve was obtained through a fatigue test on a single-point tensile-shear spot-welded specimen under constant amplitude load and finite element analysis based on the Rupp/LBF model. Fatigue analyses were performed in the time and frequency domains on the spot-welded outrigger structure, where changes in the local stress distribution and transfer function due to accumulated fatigue damage to the welding points were considered. Based on these results, it can be stated that the fatigue life of multi-point spot-welded structure under random loading should be evaluated considering the stiffness changes due to accumulated fatigue damage under the frequency domain.*

Manuscript received: May 27, 2016 / Revised: September 22, 2016 / Accepted: November 1, 2016

## 1. Introduction

Many structures are frequently exposed to random oscillating loads.<sup>1-3</sup> There are two main approaches to predicting the fatigue life of a structure under random loading: time-based and frequency-based fatigue analyses.<sup>4</sup>

Time-based quasi-static fatigue analysis is performed in the time domain by counting the cycles for a given load history in the form of stress or strain.<sup>5-8</sup> For example, Pan et al.<sup>5</sup> analyzed the stress and strain at the notch of a spot-weld nugget to propose a strain-based fatigue life prediction method for spot-weld connecting sheets of different thicknesses. Mahadevan et al.<sup>6</sup> proposed a damage tolerance reliability analysis method for spot-welded joints under multi-axial and variable amplitude loading. This quasi-static fatigue analysis has been used for various structures in the last several decades; it is convenient to use, and numerous relevant datasets are available. This quasi-static analysis requires the load time history of a structure, but obtaining the massive amount of data corresponding to the various loading cases to which a structure has been exposed is almost impossible. In addition, this method cannot consider the dynamic effect of random loads on a structure. However, vibration fatigue analysis in the frequency domain

can be utilized when the natural frequencies of structure may be within the frequency range of dynamic loads.<sup>9-12</sup> In these cases, the loading is defined in the form of the power spectral density (PSD) of excitation forces, such as acceleration, and the structural response is expressed as the frequency response, which is called a transfer function. For example, Zalaznik et al.<sup>9</sup> modified the Dirlik method to estimate the high cycle fatigue damage for uniaxial loadings resulting from random vibrations directly from power spectral analysis. Cianetti et al.<sup>10</sup> proposed an indirect method that combines the advantages of dynamic analysis conducted in the frequency domain with direct assessment criteria for fatigue in the time domain. While vibration fatigue analysis can evaluate the dynamic effect on a structure and does not need the load time history, it is not straightforward and intuitive, and it is not easy to describe fatigue damage accumulation such as crack evolution.

When spot-welded structures are exposed to an external load, they have multiple loading paths; this further improves the structural integrity.<sup>13,14</sup> Even the breakage or absence of a substantial number of spot-welds due to manufacturing defects, accidents, and fatigue damage will not critically influence the full vehicle performance. However, this approach requires a substantial safety margin for the spot-welds. In particular, because the durability is very sensitive to

spot-welds and most fatigue failures occur at or around spot-welds,<sup>5</sup> fatigue life prediction for spot-welded structures with partially broken welding points should be studied to improve the reliability of the overall structure. When some spot-welds fail, the stiffness of structure is naturally degraded,<sup>15</sup> which naturally changes the local stress distribution and eigenfrequencies of structure. Some studies have analyzed fatigue behavior by considering the change in stiffness.<sup>16-21</sup> Shang et al.<sup>16</sup> studied the effect of fatigue damage on the dynamic natural frequency response of tensile-shear spot-welded joints. They showed that relatively large changes in the natural frequency could be measured near the end of the fatigue life. Mahadevan et al.<sup>17</sup> developed a reliability-based methodology to evaluate the stiffness degradation of spot-welded joints under high levels of fatigue. They revealed that multi-point spot-welds contribute to the stiffness of a joint. Donders et al.<sup>18</sup> assessed the effect of spot-weld failure on the dynamic characteristics of a vehicle. They showed that randomly broken spot-welds reduce the stiffness of the body, which reduces the NVH (Noise, Vibration & Harshness) performance of the body. These studies mainly considered stiffness degradation and the effect of spot-weld failure on dynamic performance but did not predict the fatigue lives of spot-welded structures. Han et al.<sup>19</sup> reported on vibration fatigue analysis that considered changes in the frequency response due to fatigue damage to multi-point spot-welded joints. They revealed that changes in the eigenfrequencies greatly affect the fatigue life of a spot-welded structure. However, their study was limited to extremely simple spot-welded structures and did not consider the effect of the absence of spot-welds on the fatigue life in both the time and frequency domains.

The present study was on fatigue analysis that considers stiffness degradation from fatigue damage to a multi-point spot-welded outrigger structure utilized in an automobile engine room in the time and frequency domains.

## 2. Theoretical Background and Experiments

### 2.1 Fatigue analysis in time domain

To evaluate the fatigue life of a structure in the time domain, the stress or strain time histories are essential. Usually, stress or strain analysis can be performed through static response analysis and transient response analysis according to loads.<sup>4</sup> When the dynamic effect is negligible, quasi-static analysis does use the static structural response and load time history.

To obtain the structural response in quasi-static fatigue analysis, the results of finite element (FE) analysis for a unit input load are generally used. By combining these results and the load time history obtained through experiments or analysis, the stress or strain time history is obtained. These histories obtained are generally extremely irregular; hence, cycle counting methods such as rainflow cycle counting are generally used to get the number of stress repetitions for a certain stress amplitude and a mean stress.

When a load of one cycle acts on a structure at specific stress level, the structure received the fatigue damage  $d$ . If the stress level acts for  $N$  cycles, the fatigue damage to the structure linearly increases by  $N \times d$  (linear damage accumulation).<sup>4,5</sup> To obtain the fatigue damage per unit cycle  $d$ , the number of cycles for a certain stress amplitude and the

mean stress should be compared with the fatigue resistance of the structure under the same stress conditions; this is generally expressed as the  $S-N$  curve.

The calculated fatigue damage rates are superposed by using the Miner's rule, as given in Eq. (1). The fatigue life is identical to the reciprocal of the damage, and fatigue failure occurs when  $D = 1$ .

$$D = \sum D_i = \sum \frac{n_i}{N_i} \geq 1.0 \quad (1)$$

where  $D_i$ ,  $n_i$  and  $N_i$  are the damage fraction at the stress level  $S_i$ , number of applied cycles and fatigue life of material, respectively.

### 2.2 Fatigue analysis in frequency domain

In vibration fatigue analysis, the transfer function is defined as the structural response per unit input at each frequency of interest. And the input is expressed in the form of power spectral density (PSD) of excitation forces such as the acceleration. The PSD response at a particular location in the structure is then calculated by superposing the transfer function from the PSD of input load.

And the stress amplitude should be expressed as a probability density function (PDF)  $f_{S_a}(S_a)$  of stress amplitude, and the damage summation should be assessed as an integral.<sup>19,22</sup> To obtain a PDF from a rainflow histogram, each bin in the rainflow count has to be multiplied by  $N_i \times dS_a$ , where  $N_i$  is the total number of cycles in the histogram and  $dS_a$  is the interval width. The probability of the stress range occurring between  $S_{ai} - dS_a / 2$  and  $S_{ai} + dS_a / 2$  is given by  $f_{S_a}(S_a) \cdot dS_a$ . Hence, the number of applied cycles is  $n_i = f_{S_a}(S_a) \cdot dS_a \cdot S_i$ , and the fatigue life is  $N_i = (S_a / b)^{1/m}$ . Based on Eq. (1), the fatigue damage for time  $T$  is as follows:

$$\begin{aligned} D &= \sum \frac{n_i}{N(S_i)} = \frac{S_i}{b} \int_0^{\infty} S_a^m f_{S_a}(S_a) dS_a \\ &= \frac{E[P]T}{b} \int_0^{\infty} S_a^m f_{S_a}(S_a) dS_a \end{aligned} \quad (2)$$

where  $E[P]$  is the expected peak value of the stress time history in seconds. The symbol  $S_a$  represents the stress amplitude. The symbols  $b$  and  $m$  represent the fatigue strength and exponent, respectively, of the  $S-N$  curve.

In 1985, Dirlik proposed the empirical closed form solution for the PDF of the rainflow stress amplitude  $f_{S_a}(S_a)$ , which was found to have a wide range of applications.<sup>5,19,22</sup>

$$f_{S_a}(S_a) = \frac{\frac{D_1}{Q} \cdot e^{-\frac{Z}{Q} \times S_a} + \frac{D_2}{R^2} \cdot Z \cdot e^{-\frac{Z^2}{2R^2} \times S_a^2} + D_3 \cdot Z \cdot e^{-\frac{Z^2}{2} \times S_a^2}}{2 \cdot \sqrt{M_0}} \quad (3)$$

where

$$D_1 = \frac{2 \cdot (x_m - \gamma^2)}{b}, \quad D_2 = \frac{1 - \gamma - D_1 - D_1^2}{b} \quad (4)$$

$$D_3 = 1 - D_1 - D_2, \quad R = \frac{\gamma - x_m - D_1^2}{1 - \gamma - D_1 + D_1^2}, \quad Q = \frac{1.25 \cdot (\gamma - D_3 - D_2 \cdot R)}{D_1}$$

$$Z = \frac{1}{2 \cdot \sqrt{M_0}}, \quad \gamma = \frac{1}{\sqrt{M_0 \cdot M_4}}, \quad x_m = \frac{M_1}{M_0} \cdot \sqrt{\frac{M_2}{M_4}}$$

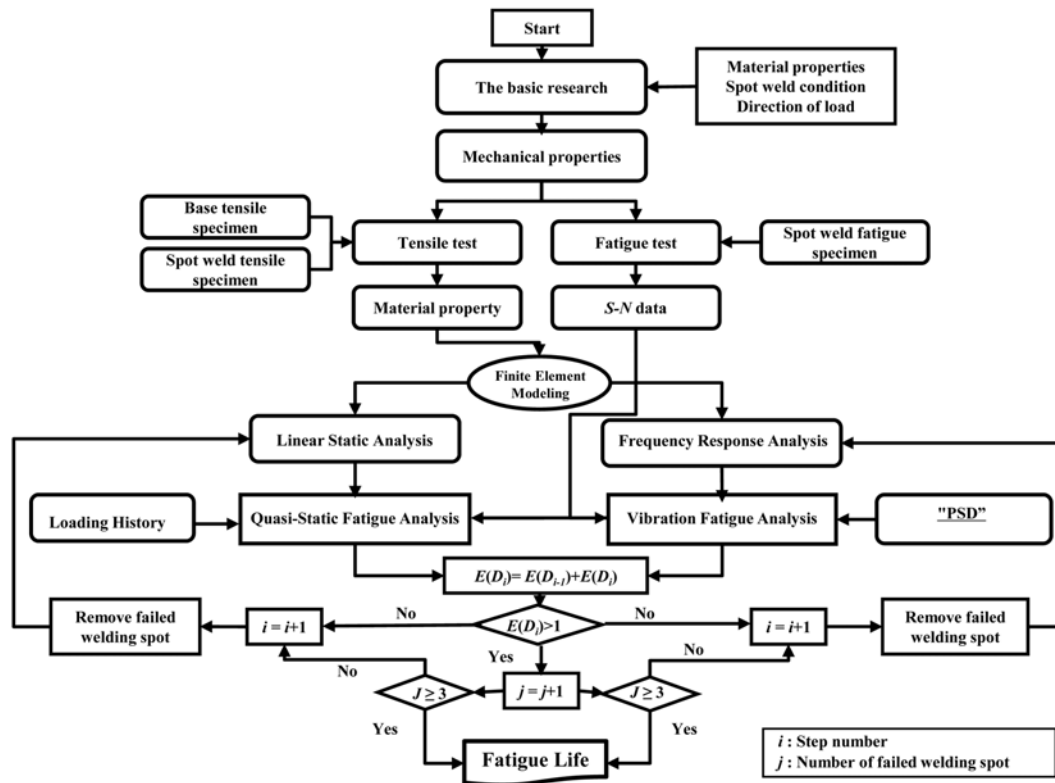


Fig. 1 Proposed quasi-static and vibration fatigue analysis

Here,  $D_1, D_2, D_3, R$  are functions of  $M_0, M_1, M_2, M_4$ . The symbols  $M_0, M_1, M_2, M_4$  are moments of the PSD about the zero frequency axis,<sup>11,19,22</sup> as shown in Eq. (4).

### 2.3 Fatigue analysis considering fatigue damage-induced stiffness degradation

For conventional quasi-static fatigue analysis in the time domain, the fatigue damage at fatigue critical locations (FCLs) is calculated by multiplying the initial local stress distribution of the damage-free structure under the unit load and load time history.<sup>8</sup> In conventional vibration fatigue analysis, the PSD response of the stress at a specific location in a structure is calculated by multiplying the initial transfer function of the structure and the PSD of the input load.<sup>9,19</sup> Here, the initial transfer function is usually obtained through FE analysis of the damage-free structure. Therefore, the initial local stress distribution and transfer function are crucial to the quasi-static and vibration fatigue analyses, respectively. It should, however, be noted, in multiple loading path structures such as spot-welded structures in automobiles, even though a single or even a substantial number of load-bearing elements may fail, the failure of the entire structure is extremely rare.<sup>20</sup> Furthermore, in actual multiple loading paths structures, the local stress distribution and transfer function may change as the stiffness degrades because of the accumulation of fatigue damage. These eventually make the change in the fatigue life of entire structure.<sup>21,23</sup> Therefore, conventional fatigue analysis methods that use the initial local stress distribution or initial transfer function may not be suitable to predicting the fatigue life of multi-point spot-welded structures with multiple loading paths.

Hence, a fatigue life assessment procedure is needed that can consider changes in the local stress distribution and transfer function due to fatigue damage accumulation. Fig. 1 presents the proposed quasi-static and vibration fatigue analysis procedure to consider changes in the local stress distribution and frequency response due to fatigue damage accumulation in a multiple loading paths structure. Here,  $i$  and  $j$  indicate the number of repetitions of the fatigue analysis and the index of fatigue damage, respectively. In this study, the number of failed spot-welded points in a spot-welded outrigger structure, which is a typical multiple loading path structure, was defined as the index of fatigue damage; hence, the fatigue damage index  $j$  is the number of failed welding points. First, a conventional time-based quasi-static and vibration fatigue analysis is conducted on the outrigger structure. The local stress distribution and transfer function obtained at this stage are termed as the initial stress distribution and transfer function, respectively. Then, the welding point that is evaluated as having the shortest fatigue life is classified as damaged, and this point is removed from the structural model in both the quasi-static and vibration fatigue analyses. The stress distribution and transfer function are reanalyzed after the damaged welding point is removed. The quasi-static and vibration fatigue analyses are reconducted using the revised stress distribution and transfer functions. This procedure is iterated until the state that is defined as failure of the whole structure is reached. To evaluate changes in the stress distribution and transfer function of the outrigger structure due to fatigue damage accumulation and the ensuing changes to the fatigue life, ASTM D 4728-06<sup>24</sup> was used to set three tiers of input load conditions in PSD form: 0.05, 0.08, and 0.11  $g^2/Hz$  (Fig. 2). The frequency range was set to 5-1000 Hz; this range covered the eigen frequencies of the

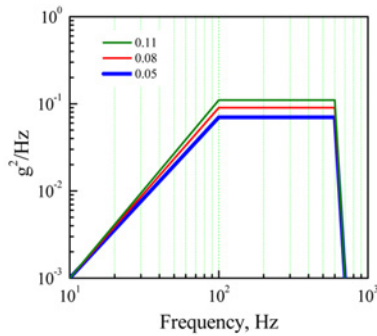


Fig. 2 Input load history for vibration fatigue analysis

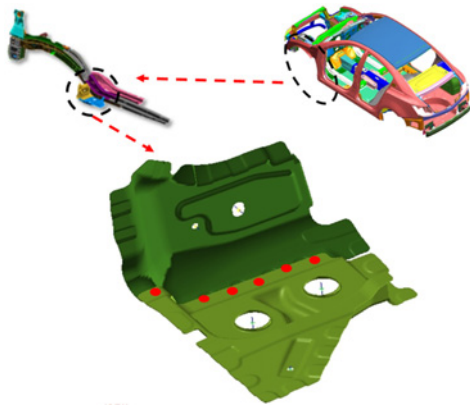


Fig. 3 Outrigger structure utilized in engine room

Table 1 Mechanical properties of galvanized steel sheet

Thickness (mm)	$E$ (GPa)	$\sigma_{ys}$ (MPa)	$\sigma_u$ (MPa)	$\epsilon$ (%)
1.3	185.76	203.09	337.14	42.62
1.4	195.30	332.73	592.14	27.52

multi-point spot-welded outrigger structure considered herein.

#### 2.4 Materials and test procedures

This study used an outrigger structure utilized in an automobile engine room (Fig. 3) as the multiple loading paths structure. This was manufactured from two galvanized steel sheets with thicknesses of 1.3 and 1.4 mm and had 6 welding points. The points were welded with an alternating current (nugget diameter: 6 mm). The welding conditions were as follows: welding current of 9.8 kA, welding time of 10 cycles, and welding force of 3450 N.

Tensile tests were conducted to measure the mechanical properties of the galvanized steel sheet used in the outrigger structure. Tensile test specimens were prepared according to ISO 6892.<sup>25</sup> Tensile tests were conducted on seven specimens under displacement control with a crosshead speed of 2 mm/min. Table 1 summarizes the results.

Under the same welding conditions used for the outrigger structure, single-point spot-welded specimens were prepared to identify the mechanical and fatigue properties of spot-welded joints according to ISO 14324,<sup>26</sup> as shown in Fig. 4. Tensile tests were conducted on seven specimens under displacement control with a crosshead speed of 2 mm/

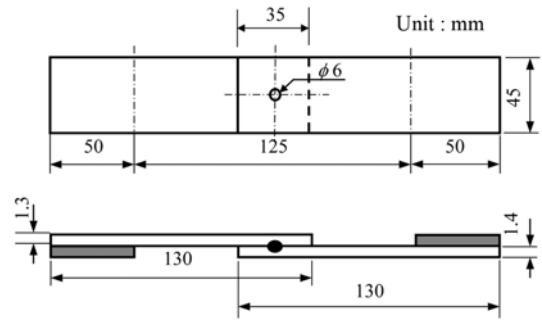


Fig. 4 Specimens for tensile and constant amplitude fatigue test

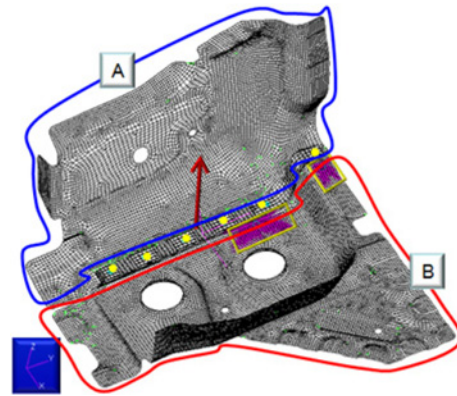


Fig. 5 FE model for outrigger structure

min.

A hydraulic fatigue testing machine (Instron model 8801, 10 tons) was used for the constant amplitude fatigue tests. The test was conducted with a sinusoidal waveform, stress ratio of  $R = 0.1$ , and test frequency of 10 Hz under a constant amplitude load according to the 14  $S-N$  method.<sup>27</sup> The fatigue limit was defined as  $3 \times 10^6$  cycles. The specimen was considered to be fractured when the length of the fatigue crack became twice that of the nugget.<sup>25</sup>

#### 2.5 FE model for outrigger structure

Static and frequency response analysis were required for the fatigue analyses in the time and frequency domains; these were performed using the MSC/Patran<sup>28</sup> and MSC/Nastran.<sup>29</sup>

The Quad4 and Tri3 shell elements were used and the spot-welding part was meshed using the Quad 4 only. Fig. 5 shows the overall model of the outrigger structure. The thicknesses of sheets A and B were 1.3 and 1.4 mm, respectively, and the mass was 1.4 kg. Here, the results given in Table 1 from the tensile test of the base material were used for the mechanical characteristics of the material.

For the FE model of the outrigger, 20,097 elements and 20,544 nodes were used. For the boundary condition, the six degrees of freedom for the edges of the upper left and lower left parts were fixed, and an inertia load of 1 g was given to the entire model. The CWELD elements, which are a specialized element for spot-welding parts in MSC/Nastran,<sup>29</sup> were used at the six spot-welding parts with nugget diameters of 6 mm.

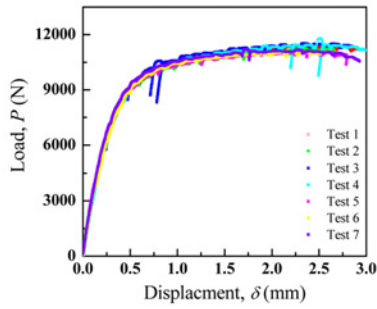


Fig. 6  $P$ - $\delta$  curve for single point spot-welded specimen

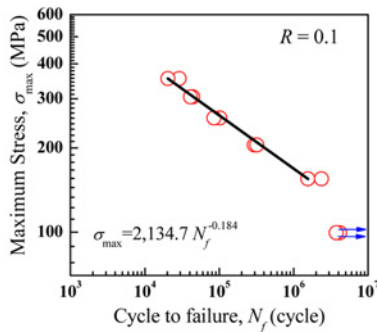


Fig. 7  $S$ - $N$  curve of single point spot-welded specimen

### 3. Results and Discussion

#### 3.1 Mechanical and fatigue behavior of base and single-point spot-welded specimen

Because spot-welded joints are affected by tensile-shear loading,<sup>30,31</sup> obtaining a fatigue stress-life curve ( $S$ - $N$  curve) directly is not straightforward. Here, an  $S$ - $N$  curve was obtained by using the load-life curve ( $P$ - $N$  curve) and FE analysis of the spot-welded joints.<sup>30,31</sup> For more details on the analysis procedure, refer to Ref. 19. The scheme is summarized as follows.

First,  $P$ - $N$  data were obtained from constant-amplitude fatigue tests for a single-point specimen, as explained in section 2.4. Second, FE analysis was conducted on actual specimens using MSC/Patran<sup>28</sup> and MSC/Nastran.<sup>29</sup> The Rupp/LBF model<sup>30,31</sup> was used to model the spot-welded specimens.

To verify the FE model for the actual specimen given above, a static test was conducted for the single-point spot-welded specimen, and its results were compared with the FE results. Fig. 6 shows the force-displacement results obtained through the static tensile test, and Table 2 compares the FE and experimental results for a given applied loads. The FE results well match with the experiment.

The radial stress at the connecting point of the nugget was obtained by correlating the loads and moments acting on the connecting elements based on the Rupp/LBF method.<sup>19</sup>

Fig. 7 exhibits the  $S$ - $N$  curve for the single-point spot-welded specimens. The following formula is for the  $S$ - $N$  curve:

$$\sigma_{max} = 2,134.7 \cdot N_f^{-0.184} \quad (5)$$

Table 2 Experimental and analysis results for single-point spot-welded specimen

Load, $P$ (kN)	Displacement, $\delta$ (mm)	
	Experiment	Analysis
4.0	0.132	0.146
5.0	0.183	0.190
6.0	0.225	0.234

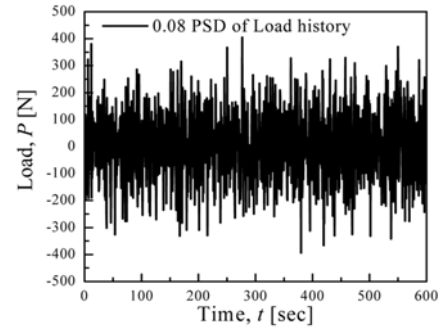


Fig. 8 Random load history for PSD = 0.08

Here,  $\sigma_{max}$  and  $N_f$  are the maximum fatigue stress applied and the fatigue life for the given stress, respectively.

#### 3.2 Fatigue analysis for spot-welded outrigger structure

##### 3.2.1 Fatigue analysis in time domain

For fatigue analysis in the time domain, load history of outrigger must be determined first. Measurements of load history in a vehicle are extremely difficult; hence, the inverse Fourier transform was applied to the PSD in Fig. 2 to produce the acceleration and resulting load time history for 600 s in the time domain. Here, the PSD levels used were 0.05, 0.08, and 0.11, respectively. Fig. 8 shows an example of produced load time history.

The load history and  $S$ - $N$  curve in Fig. 7 were used for fatigue analysis in the time domain. First, the conventional fatigue analysis method was used to calculate the fatigue life by combining the initial stress distribution and load history of the structure; the effect of stress redistribution due to damage to the spot-welding spot was not considered (i.e., no damage occurred). For a multi-point spot welded structure, damage to a single welded point does not mean the failure of entire structure. Thus, the welding point where the minimum life occurred was removed from the model, as shown by the quasi-static fatigue analysis method in Fig. 1, and the fatigue analysis was repeated until half of the total points were damaged.

Figs. 9 and 10 show the results of conventional and proposed quasi-static fatigue analysis methods, respectively. In the conventional fatigue analysis (Fig. 9), the points #2 and #3 have the shortest and longest lives, respectively. The fatigue life until three welded points were failed (i.e., the structure was completely damaged) was assessed as  $3.87 \times 10^8$  sec (i.e., almost infinite life). In contrary, when the fatigue analysis was repeated until half of the total joints were damaged, the fatigue lives of joints 2, 1, and 3 were  $1.89 \times 10^5$ ,  $1.65 \times 10^4$ , and  $3.69 \times 10^5$  sec, respectively, for a total fatigue life of  $5.75 \times 10^5$  sec. Here, the total life is summation of fatigue life for each spot weld. And it is assumed the

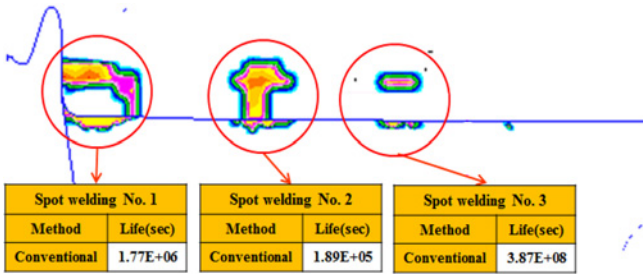


Fig. 9 Fatigue damage contour by conventional method in time domain (PSD = 0.08)

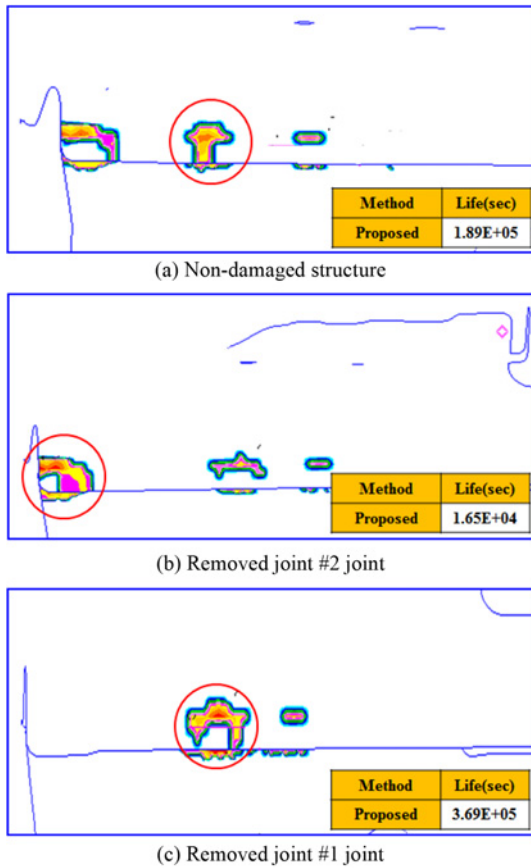


Fig. 10 Fatigue damage contour by proposed method in time domain (PSD = 0.08)

fatigue damage in non-failed point could be negligible because its fatigue damage is much less than the failed point at specific analysis run.

Table 3 summarizes the results and the fatigue lives ( $5.49 \times 10^{10}$ ,  $3.89 \times 10^8$ , and  $9.77 \times 10^7$  sec) based on conventional quasi-static fatigue analysis showed that only partial damage occurred to the structure (three out of six welding points were damaged). However, the proposed quasi-static fatigue analysis found finite fatigue lives of  $7.68 \times 10^7$ ,  $5.75 \times 10^5$ , and  $1.38 \times 10^5$  sec for the three load levels.

**3.2.2 Fatigue analysis in frequency domain**

For vibration fatigue analysis in the frequency domain, the analysis

Table 3 Comparison for results of fatigue life in time domain

Joint	PSD	Failure time (sec)					
		Proposed method			Conventional method		
		0.05	0.08	0.11	0.05	0.08	0.11
#2		2.5E+7	1.9E+5	3.6E+4	2.5E+7	1.8E+5	3.6E+4
#1		1.9E+6	1.7E+4	2.2E+3	2.2E+8	1.8E+6	3.4E+5
#3		5.0E+7	3.7E+5	9.9E+4	5.5E+10	3.9E+8	9.7E+7
Life		7.7E+7	5.8E+5	1.4E+5	5.5E+10	3.9E+8	9.7E+7

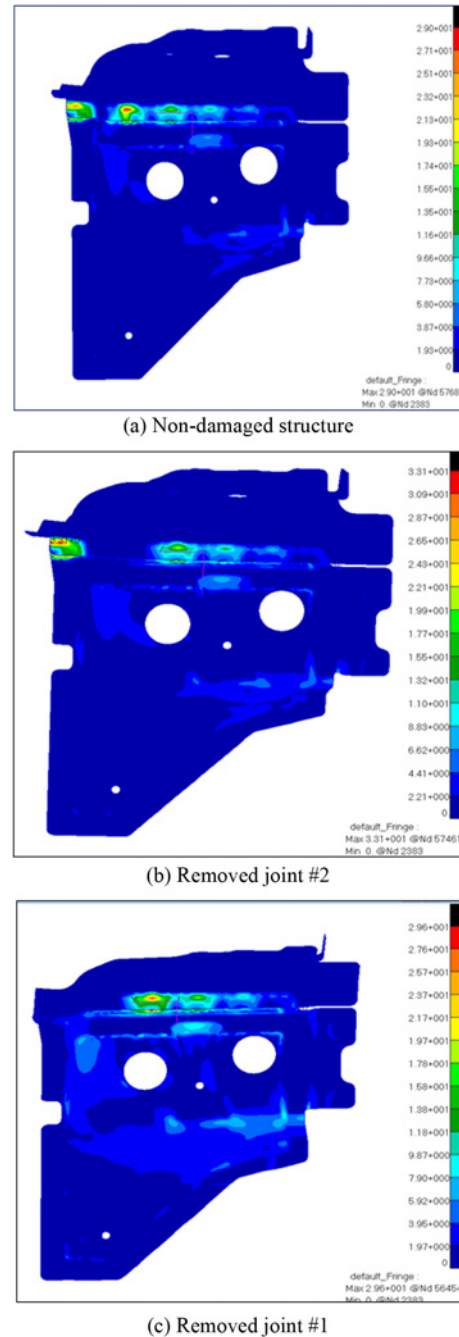


Fig. 11 Results of frequency response analysis with failed points

range and frequency increment were set to 5-1000 Hz and 10 Hz, respectively. An inertia load of 1 g was applied to the entire model. And the process shown in Fig. 1 was repeated three times until 50% of

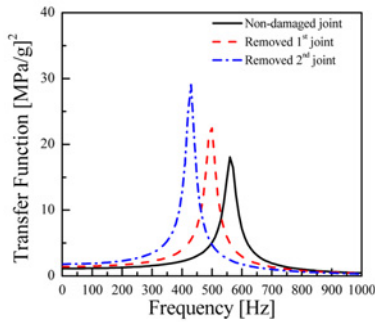


Fig. 12 Transfer functions with failed welding point

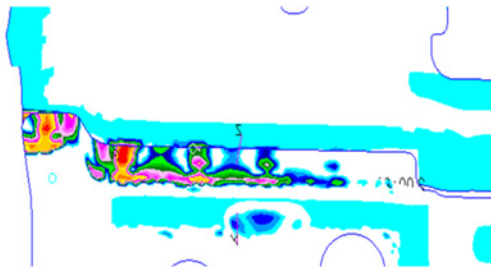


Fig. 13 Fatigue damage by conventional vibration fatigue analysis (PSD = 0.08)

the welding points were damaged.

Fig. 11 presents the results of each frequency response analysis conducted according to the above-mentioned process. The stress distribution is quite different from the damage-free structure. Fig. 12 shows the each transfer function at the third welding point (joint 3) from the left in Fig. 5. Here, we can see the natural frequencies of the welded structures are reduced as the fatigue damage evolves.

Based on the frequency response analysis results above, fatigue analysis was performed using the conventional and proposed methods. First, the conventional method (i.e., vibration fatigue analysis using the initial transfer function of undamaged structure) was performed. The initial transfer function of undamaged structure was used for all the analysis runs. Fig. 13 shows the analysis results at  $0.08 \text{ g}^2/\text{Hz}$ . At joint 2 (i.e., weakest welding point), the damage rate was  $0.000813 \text{ sec}^{-1}$ , and the fatigue life was  $1.23 \times 10^3 \text{ sec}$ . Excluding joint 2, the fatigue lives of the second and third welding points were assessed to be very long at  $5.88 \times 10^3$  and  $1.65 \times 10^5 \text{ sec}$ , respectively (total life of  $1.66 \times 10^5 \text{ sec}$ ). Identical trend was observed in the other two input PSD tiers.

To consider the changes in frequency response (transfer function) that occurred with fatigue damage accumulation, the fatigue life of the outrigger was calculated using the PSD in Fig. 2 and transfer functions in Fig. 12. Fig. 14 shows the results, which confirmed that the fatigue damage distribution of the outrigger structure changed very rapidly as the number of damaged spot-welded points increased. The fatigue lives of joints 2, 1 and 3 were assessed to be  $1.23 \times 10^3$ ,  $2.34 \times 10^2$ , and  $3.98 \times 10^3 \text{ sec}$ , respectively, for a total life of  $5.44 \times 10^3 \text{ sec}$ . Here, the total life calculation method and assumption for fatigue damage at non-failed point in analysis runs are same as those in section 3.2.1. Table 4 compares the results of the proposed and conventional analyses. The

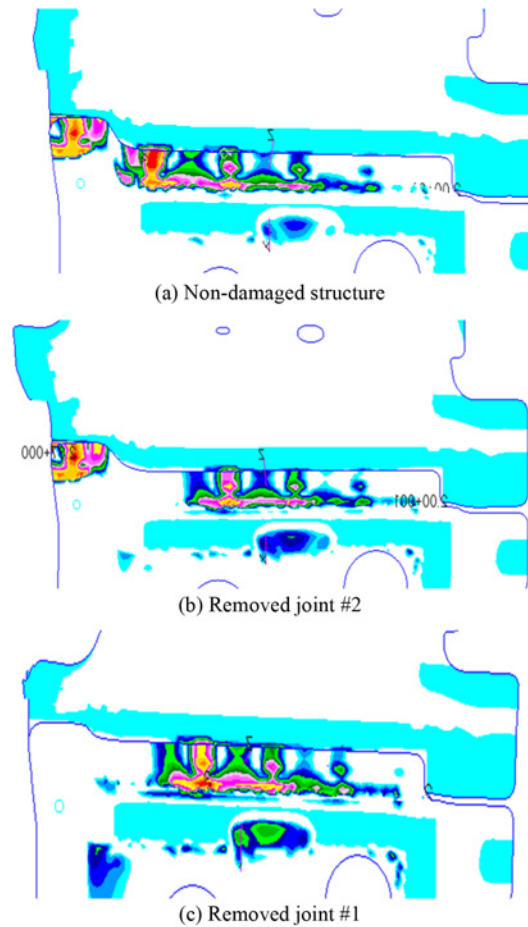


Fig. 14 Contour of fatigue damage by proposed vibration fatigue analysis method (PSD = 0.08)

Table 4 Comparison for results of fatigue life in frequency domain

Joint	PSD	Failure time (sec)					
		Proposed method			Conventional method		
		0.05	0.08	0.11	0.05	0.08	0.11
#2		1.8 E+4	1.2 E+3	2.2 E+2	1.8 E+4	1.2 E+3	2.2 E+2
#1		3.0 E+3	2.3 E+2	4.9 E+1	8.9 E+4	5.9 E+3	3.0 E+2
#3		5.9 E+4	4.0 E+3	6.9 E+2	2.8 E+6	1.7 E+5	2.7 E+5
Life		8.0 E+4	5.4 E+3	9.6 E+2	2.8 E+6	1.7 E+5	2.7 E+5

conventional fatigue analysis produced much longer fatigue lives than the proposed method. In particular, the conventional fatigue analysis can only evaluate the fatigue life of the specific welding point. But the proposed method calculated not only the fatigue lives of the specific point but the fatigue life of the entire structure including the second and third welding points.

Tables 3 and 4 present the fatigue life of the outrigger structure assessed in the time and frequency domains. The conventional analysis results using the initial stress distribution and frequency response results was considerably longer than those based on the proposed analysis process. This seems to be because the conventional process uses only the initial stress distribution and frequency response; thus, it can calculate the fatigue life of one welding point but not that of an entire structure. For the fatigue analysis results in the time and

frequency domains using the proposed process, the results in the frequency domain were found to be very conservative. This seems to be because the fatigue analysis in the frequency domain could consider the resonance of structure's eigenfrequency and excitation frequency.

When an irregular vibration load is applied to a multi-point spot welded structure, fatigue analysis in the frequency domain that considers changes in the structural response due to cumulative fatigue damage seems to be a reasonable approach.

#### 4. Conclusions

This study examined fatigue analysis methods to consider changes in the local stress distribution and degradation in the transfer function from fatigue damage to a multi-point spot-welded structure in the time and frequency domains.

(1) The mechanical properties of galvanized steel sheets were assessed through the tensile tests. A constant amplitude load control fatigue test and FE analysis were performed on spot-welded test specimens to obtain an *S-N* diagram of the spot-welded joint.

(2) The fatigue analysis in the time domain for the multi-point spot-welded outrigger structure confirmed that the local stress and fatigue life changed dramatically with the accumulation of fatigue damage.

(3) The vibration fatigue analysis considering changes in the transfer function due to fatigue damage was very conservative compared to the conventional fatigue analysis process.

(4) It could be stated that the vibration fatigue analysis that considered changes in the response of spot-welded structure due to fatigue damage is the best reasonable approach under irregular vibration loads.

#### ACKNOWLEDGEMENT

This work was supported by a Human Resources Development of the Korea Institute of Energy Technology Evaluation and Planning (KETEP) grant funded by Ministry of Trade, Industry & Energy (No. 20144030200590) and Basic Science Research Program through the National Research Foundation of Korea (NRF) funded by the Ministry of Education (NRF-2016R1A6A1A0301 3567).

#### REFERENCES

- Bonte, M. H. A., De Boer, A., and Liebrechts, R., "Determining the Von Mises Stress Power Spectral Density for Frequency Domain Fatigue Analysis Including Out-of-Phase Stress Components," *Journal of Sound and Vibration*, Vol. 302, No. 1, pp. 379-386, 2007.
- He, C., Huang, C., Liu, Y., and Wang, Q., "Fatigue Damage Evaluation of Low-Alloy Steel Welded Joints in Fusion Zone and Heat Affected Zone Based on Frequency Response Changes in Gigacycle Fatigue," *International Journal of Fatigue*, Vol. 61, No. pp. 297-303, 2014.
- Jin, J.-W., Kang, K.-W., and Kim, J.-H., "Development of Durability Test Procedure of Vibration-Based Energy Harvester in Railway Vehicle," *Int. J. Precis. Eng. Manuf.-Green Tech.*, Vol. 2, No. 4, pp. 353-358, 2015.
- Moon, S.-I., Cho, I.-J., and Yoon, D., "Fatigue Life Evaluation of Mechanical Components Using Vibration Fatigue Analysis Technique," *Journal of Mechanical Science and Technology*, Vol. 25, No. 3, pp. 631-637, 2011.
- Pan, N. and Sheppard, S., "Spot Welds Fatigue Life Prediction with Cyclic Strain Range," *International Journal of Fatigue*, Vol. 24, No. 5, pp. 519-528, 2002.
- Mahadevan, S. and Ni, K., "Damage Tolerance Reliability Analysis of Automotive Spot-Welded Joints," *Reliability Engineering & System Safety*, Vol. 81, No. 1, pp. 9-21, 2003.
- Lee, Y.-L., Raymond, M. N., and Villaire, M. A., "Durability Design Process of a Vehicle Suspension Component," *Journal of Testing and Evaluation*, Vol. 23, No. 5, pp. 354-363, 1995.
- Chu, C.-C., "Multiaxial Fatigue Life Prediction Method in the Ground Vehicle Industry," *International Journal of Fatigue*, Vol. 19, No. 93, pp. 325-330, 1997.
- Zalaznik, A. and Nagode, M., "Frequency Based Fatigue Analysis and Temperature Effect," *Materials & Design*, Vol. 32, No. 10, pp. 4794-4802, 2011.
- Braccesi, C., Cianetti, F., Lori, G., and Pioli, D., "Evaluation of Mechanical Component Fatigue Behavior Under Random Loads: Indirect Frequency Domain Method," *International Journal of Fatigue*, Vol. 61, pp. 141-150, 2014.
- Haiba, M., Barton, D. C., Brooks, P. C., and Levesley, M. C., "Review of Life Assessment Techniques Applied to Dynamically Loaded Automotive Components," *Computers & Structures*, Vol. 80, No. 5, pp. 481-494, 2002.
- Kang, B., Sin, H.-C., and Kim, J., "Optimal Shape Design of the Front Wheel Lower Control Arm Considering Dynamic Effects," *International Journal of Automotive Technology*, Vol. 8, No. 3, pp. 309-317, 2007.
- Radaj, D., "Review of Fatigue Strength Assessment of Nonwelded and Welded Structures Based on Local Parameters," *International Journal of Fatigue*, Vol. 18, No. 3, pp. 153-170, 1996.
- Zhang, W., Roy, G., Elmer, J., and DebRoy, T., "Modeling of Heat Transfer and Fluid Flow During Gas Tungsten Arc Spot Welding of Low Carbon Steel," *Journal of Applied Physics*, Vol. 93, No. 5, pp. 3022-3033, 2003.
- Zhang, Y. and Taylor, D., "Optimization of Spot-Welded Structures," *Finite Elements in Analysis and Design*, Vol. 37, No. 12, pp. 1013-1022, 2001.
- Shang, D.-G., Barkey, M. E., Wang, Y., and Lim, T. C., "Effect of Fatigue Damage on the Dynamic Response Frequency of Spot-Welded Joints," *International Journal of Fatigue*, Vol. 25, No. 4, pp. 311-316, 2003.



17. Mahadevan, S., Hollander, B., Ni, K., and Mao, H., "Spot-Weld Joint Stiffness Degradation Under High Mileage: Probabilistic Analysis," SAE Technical Paper, No. 2003-01-0694, 2003.
18. Donders, S., Brughmans, M., Hermans, L., Liefvooghe, C., Van der Auweraer, H., and Desmet, W., "The Robustness of Dynamic Vehicle Performance to Spot Weld Failures," *Finite Elements in Analysis and Design*, Vol. 42, No. 8, pp. 670-682, 2006.
19. Han, S.-H., An, D.-G., Kwak, S.-J., and Kang, K.-W., "Vibration Fatigue Analysis for Multi-Point Spot-Welded Joints Based on Frequency Response Changes due to Fatigue Damage Accumulation," *International Journal of Fatigue*, Vol. 48, pp. 170-177, 2013.
20. Wang, R.-J., Shang, D.-G., Li, L.-S., and Li, C.-S., "Fatigue Damage Model Based on the Natural Frequency Changes for Spot-Welded Joints," *International Journal of Fatigue*, Vol. 30, No. 6, pp. 1047-1055, 2008.
21. Wang, R.-J. and Shang, D.-G., "Fatigue Life Prediction Based on Natural Frequency Changes for Spot Welds Under Random Loading," *International Journal of Fatigue*, Vol. 31, No. 2, pp. 361-366, 2009.
22. Dirlik, T., "Application of Computers in Fatigue Analysis," Ph.D. Thesis, University of Warwick, 1985.
23. Tani, I., Lenoir, D., and Jezequel, L., "Effect of Junction Stiffness Degradation due to Fatigue Damage of Metallic Structures," *Engineering Structures*, Vol. 27, No. 11, pp. 1677-1688, 2005.
24. ASTM D 4728-06, "Standard Test Method for Random Vibration Testing of Shipping Containers," 2012.
25. ISO 6892-1, "Metallic Materials - Tensile Testing - Part 1: Method of Test at Room Temperature," 2016.
26. ISO 14324, "Resistance Spot Welding - Destructive Tests of Welds - Method for the Fatigue Testing of Spot Welded Joints," 2003.
27. JSME S002, "Standard Method of Statistical Fatigue Testing," 1981.
28. MSC Software, "Patran 2012 User's Guide," Docs ID: DOC10145, 2012.
29. MSC Software, "MSC Nastran Linear Static Analysis User's Guide," Docs ID: DOIC 10003, 2012.
30. Rupp, A., Störzel, K., and Grubisic, V., "Computer Aided Dimensioning of Spot-Welded Automotive Structures," SAE Technical Paper, No. 950711, 1995.
31. Gao, Y., Chucas, D., Lewis, C., and McGregor, I. J., "Review of CAE Fatigue Analysis Techniques for Spot-Welded High Strength Steel Automotive Structures," SAE Technical Paper, No. 2001-01-0835, 2001.